A Safe and Sensitive Antiviral Screening Platform Based on Recombinant Human Coronavirus OC43 Expressing the Luciferase Reporter Gene

Liang Shen[1], Yang Yang[1], Fei Ye[1], Gaoshan Liu[1], Marc Desforges[2], Pierre J. Talbot[2, *], Wenjie Tan[1, *]

1 Key Laboratory of Medical Virology, Ministry of Health, National Institute for Viral Disease Control and Prevention, China CDC, Beijing 102206, China;

2. Laboratory of Neuroimmunovirology, INRS-Institut Armand-Frappier, Université du Québec, Laval, Québec, Canada.

Running title: Recombinant HCoV- OC43 Expressing Reporter

[*] **Corresponding Authors**: Wenjie Tan, Key Laboratory of Medical Virology, Ministry of Health, National Institute for Viral Disease Control and Prevention, China CDC 155 Changbai Road, ChangPing District, Beijing 102206, China, Tel/ Fax: 86-10-5890 0878, E-mail: tanwj28@163.com; Pierre J. Talbot, Laboratory of Neuroimmunovirology, INRS-Institut Armand-Frappier, Université du Québec, Laval, Québec, Canada, E-mail: pierre.talbot@iaf.inrs.ca

Abstract

Human coronaviruses (HCoVs) cause 15–30% of mild upper respiratory tract infections. However, no specific antiviral drugs are available to prevent or treat HCoV infections to date. Here, we developed four infectious recombinant HCoVs-OC43 (rHCoVs-OC43), which express the Renilla luciferase (Rluc) reporter gene. Among these four rHCoVs-OC43, rOC43-ns2DelRluc (generated by replacing ns2 with the Rluc gene) showed robust luciferase activity with only a slight impact on its growth characteristics. Additionally, this recombinant virus remained stable for at least 10 passages in BHK-21 cells. The rOC43-ns2DelRluc was comparable with its parental wild-type virus (HCoV-OC43-WT) with respect to the quantity of the antiviral activity of chloroquine and ribavirin. We showed that chloroquine strongly inhibited HCoV-OC43 replication *in vitro*, with an IC_{50} of 0.33 μM. However, ribavirin showed inhibition on HCoV-OC43 replication only at high concentrations which may not be applicable to humans in clinical treatment, with an IC_{50} of 10 μM. Furthermore, using a luciferase-based small interfering RNA (siRNA) screening assay, we identified double-stranded RNA-activated protein kinase (PKR) and DEAD-box RNA helicases (DDX3X) that exhibited antiviral activities, which were further verified by the use of HCoV-OC43-WT. Therefore, rOC43-ns2DelRluc represents a promising safe and sensitive platform for high throughput antiviral screening and quantitative analysis of viral replication.

41 **Introduction**

42 Coronaviruses (CoVs) belong to the family *Coronaviridae* in the order
43 *Nidovirales* (1). They have a positive-sense RNA genome ~30 kb in length, the largest
44 found in any RNA viruses. CoVs infect avian species and a wide range of mammals,
45 including humans (2). Currently, six CoVs that are able to infect humans have been
46 identified; four circulating strains HCoV-229E, -OC43, -HKU1, NL63 and two
47 emergent strains severe acute respiratory syndrome coronavirus (SARS-CoV) and
48 Middle East respiratory syndrome coronavirus (MERS-CoV). Indeed, in 2003, an
49 outbreak of severe acute respiratory syndrome (SARS) first demonstrated the
50 potentially lethal consequences of zoonotic CoV infections in humans. In 2012, a
51 similar, previously unknown CoV emerged, MERS-CoV, which has thus far caused
52 over 1,650 laboratory-confirmed infections, with a mortality rate of about 30% (3, 4).
53 However, to date, no effective drug has been identified for the treatment of HCoV
54 infections and few host factors have been identified that restrict the replication of
55 HCoV. The emergence of these highly pathogenic HCoVs has reignited interest in
56 studying HCoV biology and virus-host interactions. Therefore, a safe and sensitive
57 screening model is required for rapid identification of potential drugs and screening
58 antiviral host factors capable of inhibiting HCoV infection.

59 The introduction of a reporter gene into the viral genome provides a powerful
60 tool for initial rapid screening and evaluation of antiviral agents. The unique CoV
61 transcription mechanism allows efficient expression of reporter genes by inserting
62 reporter genes under the control of transcription regulatory sequence (TRS) elements.

To date a number of reporter CoVs have been generated (5–11) and several reporter CoVs have been applied to antivirals screening assay (10-14), but most of them are animal CoVs which cause disease in only one animal species and are generally not susceptible to humans. Among these reporter CoVs, only one reporter CoV (SARS-CoV-GFP) was based on HCoV and applied to a small interfering RNA (siRNA) library screening (14). However, the SARS-CoV-GFP assay lacks sensitivity and requires a high infectious dose (multiplicity of infection [MOI] of 10) for quantitative screening. Moreover, experiments with this reporter virus require a BSL-3 facility, which is costly and labor-intensive. Thus, it is critical to generate a safe and sensitive reporter HCoV for high-throughput screening (HTS) assays. Moreover, generation of a reporter HCoV was more suitable to screen drugs for clinical treatment than the reporter animal CoVs. HCoV-OC43 shows promise as a reporter virus for screening anti-HCoVs drugs or identifying host factors. HCoV-OC43 was first isolated from a patient with upper respiratory tract disease in the 1960s, together with severe Beta-CoVs (SARS-CoV and MERS-CoV), all belong to the *Betacoronavirus* genus (15, 16), and these three virus strains have a high level of conservation for some essential functional domains, especially within 3CLpro, RdRp, and the RNA helicase, which represent potential targets for broad-spectrum anti-HCoVs drug design (17, 18). Moreover, unlike SARS-CoV or MERS-CoV, HCoV-OC43 usually causes a mild respiratory tract disease and can be used for screening antivirals in a BSL-2 facility. Furthermore, a small animal model of HCoV-OC43 has been developed and used successfully for antiviral trials (18, 19).

HCoV-OC43 encodes two accessory genes, ns2 and ns12.9 (20). The ns2 gene, located between nsp13 and HE gene loci, encodes a protein of unknown function. The ns12.9 gene, located between the S and E structural genes, encodes a protein that was recently demonstrated as a viroporin involved in HCoV-OC43 morphogenesis and pathogenesis (21). In this study, four infectious recombinant HCoVs-OC43 (rHCoVs-OC43) were generated based on the ATCC VR-759 strain of HCoV-OC43 by genetic engineering of the two accessory genes. Successfully rescued viruses were characterized and subsequently investigated for genetic stability. One reporter virus, rOC43-ns2DelRluc, showed robust Rluc activity and had similar growth kinetics to the parental wild-type HCoV-OC43 (HCoV-OC43-WT). Furthermore, this reporter virus was used successfully to evaluate the antiviral activity of Food and Drug Administration (FDA)-approved drugs and siRNA screening assays. Our study indicated that the replacement of accessory ns2 gene represents a promising target for the generation of reporter HCoV-OC43 and provides a useful platform for identifying anti-HCoVs drugs and host factors relevant to HCoV replication.

Materials and methods

Plasmid construction. The infectious full-length cDNA clone pBAC-OC43^{FL} (22), containing a full-length cDNA copy of the HCoV-OC43, was used as the backbone to generate four rHCoVs-OC43 (Fig. 1). The Rluc gene was amplified from pGL4.75hRluc/CMV vector (Promega) and introduced into the plasmid pBAC-OC43^{FL} by standard overlapping polymerase chain reaction (PCR). Modified

fragments of HCoV-OC43 cDNA, for replacing the ns2 gene with Rluc gene (between 21,523 and 22,915 nucleotides, inclusively) or in-frame insertion of the Rluc gene into the ns2 gene (between nucleotides 21,517 and 21,518, inclusively), were generated by overlapping PCR and cloned into *Nar*I/*Pme*I-digested pBAC-OC43^{FL} to generate pBAC-OC43-ns2DelRluc or pBAC-OC43-ns2FusionRluc. The same strategies were employed for replacing the ns12.9 gene with Rluc gene or in-frame insertion of the Rluc gene into the ns12.9 gene, resulting in plasmids pBAC-OC43-ns12.9StopRluc and pBAC-OC43-ns12.9FusionRluc, respectively. Further details are available on request. All final constructs were verified by Sanger sequencing.

Cells and antibodies. BHK-21, HEK-293T, and Huh7 cells were grown in Dulbecco's modified Eagle medium (DMEM) (Gibco) supplemented with 10% fetal bovine serum (FBS) (Gibco), 2 mM L-glutamine (Sigma-Aldrich) and incubated at 37°C with 5% CO_2.

The anti-Renilla luciferase (ab185925), anti-PKR (ab32052) and anti-phosphorylated PKR (ab81303) rabbit monoclonal antibodies were purchased from Abcam. The anti-Flag (F7425) rabbit polyclonal antibody was purchased from Sigma-Aldrich. The anti-eIF2α (D7D3), anti-phosphorylated-eIF2α (Ser51) (D9G8), anti-DDX3X (D19B4) and anti-β-actin (13E5) rabbit monoclonal antibodies were obtained from Cell Signaling Technology. The infrared IRDye 800CW-labeled goat anti-mouse IgG (H+L) and IRDye 680RD goat anti-rabbit IgG were purchased from LI-COR Biosciences.

Generation and titration of recombinant viruses. The reporter viruses

129 rOC43-ns2DelRluc, rOC43-ns2FusionRluc, rOC43-ns12.9StopRluc and
130 rOC43-ns12.9FusionRluc were rescued from the infectious cDNA clones
131 pBAC-OC43-ns2DelRluc, pBAC-OC43-ns2FusionRluc, pBAC-OC43-
132 ns12.9StopRluc and pBAC-OC43-ns12.9FusionRluc, respectively. In brief, BHK-21
133 cells grown to 80% confluence were transfected with 4 µg of pBAC-OC43^{FL},
134 pBAC-OC43-ns2DelRluc, pBAC-OC43-ns2FusionRluc,
135 pBAC-OC43-ns12.9StopRluc or pBAC-OC43-ns12.9FusionRluc using the
136 X-tremeGENE HP DNA Transfection Reagent (Roche) according to the
137 manufacturer's instructions. After incubation for 6 h at 37°C in a humidified 5% CO_2
138 incubator, the transfected cells were washed three times with DMEM and maintained
139 in DMEM supplemented with 2% FBS for 72 h at 37°C and an additional 96 h at
140 33°C. Next, the rHCoVs-OC43 were harvested by three freeze-thaw cycles followed
141 by centrifugation at 2,000 × *g* for 20 min at 4°C. The HCoV-OC43-WT was obtained
142 from the full-length cDNA clone pBAC-OC43^{FL}. All viruses were propagated in
143 BHK-21 cells in DMEM supplemented with 2% FBS.

144 The titers of rHCoVs-OC43 were determined by indirect immunofluorescence
145 assay (IFA). Briefly, BHK-21 cells in 96-well plates were infected with 10-fold
146 diluted viruses. The viral titers were determined at 72 h post-infection (hpi) by IFA
147 and expressed as median tissue culture infective dose ($TCID_{50}$)/mL, according to the
148 Reed and Münch method (23).

149 **Determination of viral growth kinetics.** BHK-21 cells seeded on 48-well plates
150 were infected with HCoV-OC43-WT or rHCoVs-OC43 at an MOI of 0.01. After 2 h

of incubation at 33°C, cells were washed with PBS, and replaced with fresh medium before incubation at 33°C. The supernatants (150 µL) were harvested at 24, 48, 72, 96, 120, 144 and 168 hpi, and 150 µL of fresh media were added to the cells. The titer for each virus at the indicated time point was determined by IFA, as described above.

Rluc activity assay. Analysis of Rluc expression was performed in 48- or 96-well plates. Briefly, BHK-21 cells or HEK-293T cells in plates were infected with rHCoVs-OC43 at an MOI of 0.01. At the various time-points post-infection, the cells in each well were assayed for relative light units (RLUs) using the Renilla-Glo Luciferase Assay System (Promega) according to the manufacturer's instructions.

Dual luciferase reporter assay system. HEK-293T cells were seeded in 24-well plates at a cell density of 2.5×10^5 cells per well. The next day, cells were transfected with plasmids expressing DDX3X or TBK1 (150 or 300 ng), along with IFN-β-Luc and Rluc internal reference reporter plasmids. At 24 h post-transfection, cells were lysed and analyzed with the Dual-Luciferase Reporter Assay System (Promega) according to the manufacturer's protocol.

Western blot analysis. Infected or uninfected cells were washed twice with PBS, lysed with NP-40 buffer (50 mM Tris [pH 7.5], 150 mM NaCl, 0.5% NP-40, and 0.5 mM EDTA) containing 1 mM phenylmethylsulfonyl fluoride (PMSF) and 1 mg/mL protease inhibitor cocktail (Roche) for 30 min at 4°C. An equal volume of each sample was separated by sodium dodecyl sulfate-polyacrylamide gel electrophoresis (SDS-PAGE) and transferred to nitrocellulose membranes (Pall). The membranes were blocked with 5% skim milk in PBS containing 0.5% Tween (PBST) for 1 h at

173 room temperature and incubated with primary antibody overnight at 4°C. After
174 washes with PBST, the membranes were further incubated for 1 h with infrared
175 IRDye 800CW-labeled goat anti-mouse IgG (H+L) (1:10,000) (LI-COR) or IRDye
176 680RD goat anti-rabbit IgG (H+L) (1:10,000) (LI-COR), blots were scanned on the
177 Odyssey Infrared Imaging System (LI-COR).

178 **RNA isolation and reverse transcription PCR (RT-PCR).** Total RNA was
179 extracted from virus-infected BHK-21 cells using TRIzol reagent (Invitrogen) and
180 treated with DNase I to remove potential genomic DNA. The RNA concentration was
181 quantified using a NanoDrop 2000 Series spectrophotometer (Thermo Scientific). For
182 RT-PCR, two sets of primer pairs flanking the inserted reporter gene were used: one
183 pair for rOC43-ns2FusionRluc and rOC43-ns2DelRluc (5′-GTG TAA GCC CAA
184 GGT TGA GAT AG-3′) / (5′-GTC GTT CAG ATT GTA ATC ATA TTG -3′), and
185 another for rOC43-ns129FusionRluc and rOC43-ns129DelRluc (5′-CAT ATG AAT
186 ATT ATG TAA AAT GGC -3′)/ (5′-GCC ATA AAC ATT TAA CTC CTG TC -3′). The
187 PCR products were subjected to electrophoresis on a 1% agarose gel.

188 **Real-time PCR.** Semi-quantitative PCR was performed using the One Step
189 SYBR PrimeScript RT-PCR Kit (Takara) according to the manufacturer's instructions.
190 Fold-induction values were calculated using the $2^{-\Delta\Delta Ct}$ method and mRNA expression
191 was normalized to GAPDH. Genomic RNA copies of HCoV-OC43-WT or
192 rOC43-ns2DelRluc was quantified using a previously described quantitative RT-PCR
193 as described previously (24). All primers are available in Table S1.

194 **Stability of rHCoVs-OC43.** To examine the stability of the inserted Rluc genes,

rHCoVs-OC43 and their parental HCoV-OC43-WT were passaged 13 times in BHK-21 cells (Fig. 3A). Briefly, cells in a 25-cm^2 flask were infected with the rescued rHCoVs-OC43 and HCoV-OC43-WT (defined as P0) at an MOI of 0.01. At 120 hpi, 300 μL of cell culture supernatants from the passaged virus (P1) were added to naïve cells to generate passage 2 virus (P2). After 13 rounds of serial passage, viral RNA was extracted from the supernatant of infected cells of each passage (P0 to P13) and the stability of the inserted reporter genes was detected by RT-PCR as described above and cloned into the pMD18-T vector (Takara) for Sanger sequencing (four clones were sequenced for each passage). The titers of rHCoVs-OC43 from P1 to P13 were determined using IFA. In addition, BHK-21 cells in 48-well plates were infected with each passage of rHCoVs-OC43 at an MOI of 0.01 and measured the Rluc activity at 72 hpi using the Renilla-Glo Luciferase Assay System.

Cell viability assay. The cell viability assay was performed using a Cell Titer-Glo Luminescent Cell Viability Assay kit (Promega). Briefly, cells were seeded in 96-well plates in triplicate. After 24 h, various concentrations of chloroquine (0–80 μM) and ribavirin (0–320 μM) (Sigma-Aldrich) were added to the medium. At 72 h, the plates were equilibrated at room temperature for 60 min, and 100 μL of Celltiter-Glo reagent was added to the medium. The plates were subsequently shaken on a shaker for 2 min to induce cell lysis. After a final incubation for 10 min at room temperature, the luminescence was measured using a GLOMAX Luminometer system (Promega).

Antiviral drug assay. For the viral RNA load-based antiviral assay, confluent

BHK-21 cells in 48-well culture plates were infected in triplicate with HCoV-OC43-WT or rOC43-ns2DelRluc at an MOI of 0.01. After 2 h adsorption at 33°C, the inoculum was removed and the cells were washed three times with DMEM. Subsequently, complete DMEM containing various concentrations of chloroquine (0–80 μM) or ribavirin (0–320 μM) were added to the cells. Cells were incubated for 72 h at 33°C in a humidified 5% CO_2 incubator. The supernatants of cells infected with HCoV-OC43-WT or rOC43-ns2DelRluc were collected, and the viral RNA loads were determined using quantitative RT-PCR as described above. For the luciferase-based antiviral assay, BHK-21 cells in 96-well culture plates were infected with rOC43-ns2DelRluc followed by incubation with chloroquine or ribavirin for 72 h; then the Rluc activity was measured as described above.

RNA interference (RNAi) screening. We designed siRNA pools targeting eight potential host antiviral restriction factors for screening, and each individual siRNA pool consisted of three siRNAs targeting the same gene. A non-targeting siRNA having no matches to the viral or human genome served as a blank control. The specific siRNAs targeting antiviral host factors were synthesized by GenePharma (sequences provided upon request).

For testing of siRNA pools, HEK-293T cells plated in poly-L-lysine (PLL)-coated 48-well plates were transfected with siRNA pools using X-tremeGene siRNA Transfection Reagent (Roche) at a final concentration of 300 nM. After incubation for 24 h, cells were subsequently infected in triplicate with rOC43-ns2DelRluc at an MOI of 0.01. At 60 hpi, the Rluc activity was measured as

described above.

Mice and infection. 12-day-old female BALB/c mice (Animal Care Centre, Chinese Academy of Medical Science, Beijing, China) were randomly distributed into three groups. Two groups were intracerebral inoculation (IC) with 20 μl of DMEM containing 100 $TCID_{50}$ of HCoV-OC43-WT or rOC43-ns2DelRluc and another group was intracerebral inoculation with 20 μl of DMEM. The infected mice were monitored for survival. For the passages of rOC43-ns2DelRluc in BALB/c mice, 12-day-old mice were intracerebral inoculation with 500 $TCID_{50}$ of rOC43-ns2DelRluc (P0) in 20 μl of DMEM and sacrificed at 3 days post-inoculation, brains were homogenized in 500 μl of PBS containing 100 U/ml penicillin, 0.1 mg/ml streptomycin and 0.5 μg/ml amphotericin B. Then Brain homogenate were clarified by low-speed centrifugation at 3,000 rpm for 12 min to obtain passage 1 virus (P1). After 5 rounds of serial passages, the rOC43-ns2DelRluc was passaged to P5.

Statistical analysis. Differences between groups were examined for statistical significance using Student's *t*-test. Confidence levels are indicated in the figures as follows: *, $P < 0.05$; **, $P < 0.01$.

Results

Characterization of rHCoVs-OC43 expressing Rluc. Reporter virus is a valuable screening tool for identifying novel antiviral drugs or host factors. To generate a high expression reporter HCoV-OC43 and evaluate the roles of ns2 and ns12.9 genes in viral production, four rHCoVs-OC43 were obtained following

261 replacement of the ns2 or ns12.9 genes with Rluc (rOC43-ns2DelRluc and
262 rOC43-ns12.9StopRluc) or in-frame insertion of the Rluc gene into ns2 or ns12.9
263 genes (rOC43-ns2FusionRluc and rOC43-ns12.9FusionRluc), respectively (Fig. 1).

264 The *in vitro* growth characteristics of the reporter viruses were analyzed by
265 growth kinetics in BHK-21 cells. rOC43-ns2FusionRluc and
266 rOC43-ns12.9FusionRluc showed replication kinetics similar to that of
267 HCoV-OC43-WT, reached a peak titer of 10^6 $TCID_{50}$/mL at 144 hpi (Fig. 2B),
268 indicating that ns2-Rluc or ns12.9-Rluc fusion proteins were likely to retain their
269 biological functions in the life cycle of HCoV-OC43. Moreover, the viral titer of
270 rOC43-ns2DelRluc was only 4-fold lower than that of HCoV-OC43-WT at 144 hpi,
271 indicating that the ns2 gene is nonessential for virus replication (Fig. 2B). By contrast,
272 rOC43-ns12.9StopRluc showed impaired growth kinetics, with a peak titer of $10^{4.8}$
273 $TCID_{50}$/mL at 144 hpi, which was ~27-fold lower than that of the parental
274 HCoV-OC43-WT (Fig. 2B). This result indicated that the ns12.9 viroporin is
275 important for viral propagation in cell culture. To further explore whether the
276 reduction in virus titers of rOC43-ns2DelRluc was due to the abolishment of ns2
277 protein expression, we performed a transient complementation assay. An ns2 protein
278 expression vector was constructed, and its expression levels were detected by Western
279 blot analysis (Fig. 2C, left). Compared with the empty vector-transfected cells,
280 ns2-expressing cells exhibited a slight increase in virus titers for HCoV-OC43-WT
281 (Fig. 2C, right). These results confirmed that the loss of infectious virus production by
282 deletion of ns2 gene could be compensated by transient expression of ns2 in BHK21

cells.

Rluc activity in cells infected with reporter viruses was also characterized. Surprisingly, the viral titer of rOC43-ns2DelRluc was 4-fold lower than that of the rOC43-ns2FusionRluc at 144 hpi, but showed robust Rluc expression levels, with Rluc activity 18-fold higher than that of the rOC43-ns2FusionRluc (Fig. 2D). rOC43-ns12.9StopRluc, although having impaired growth kinetics, showed relatively high Rluc activity, with 10^7 RLUs at 144 hpi. However, rOC43-ns12.9FusionRluc showed faint Rluc activity even though it showed similar replication kinetics with HCoV-OC43-WT (Fig. 2D). Moreover, Western blotting was performed to confirm the Rluc expression levels of the reporter viruses at 72 and 96 hpi. The results showed similar expression levels of N proteins in rOC43-ns2FusionRluc and rOC43-ns2DelRluc, but the expression of ns2-Rluc fusion protein of rOC43-ns2FusionRluc was significantly reduced compared with Rluc proteins of rOC43-ns2DelRluc (Fig. 2E). In addition, we observed high levels of Rluc proteins in the lysates of cells infected with rOC43-ns12.9StopRluc, but no ns12.9-Rluc fusion proteins were detected in the lysates of rOC43-ns12.9FusionRluc-infected cells, perhaps due to its low Rluc expression levels at 96 hpi (Fig. 2F). These results correlated with the Rluc activity detected at the corresponding hpi (Fig. 2D).

These observations prompted us to ascertain whether replacement of ns2 or ns12.9 with Rluc gene could enhance the subgenomic (sg) mRNA transcription efficiency when compared with that of ns2-Rluc or ns12.9-Rluc fusion genes, we detected the transcription levels of ns2 (HCoV-OC43-WT), Rluc (rOC43-ns2DelRluc

or rOC43-ns12.9StopRluc), ns2-Rluc fusion (rOC43-ns2FusionRluc) and ns12.9-Rluc fusion (rOC43-ns12.9FusionRluc) genes using semi-quantitative PCR. The sg mRNA level of Rluc (rOC43-ns2DelRluc) was only 2.3-fold higher than that of ns2 of HCoV-OC43-WT, and was similar to the sg mRNA level of the ns2-Rluc fusion gene (Fig. 2G). Moreover, replacement of ns12.9 gene with Rluc gene or insertion of Rluc gene in frame into the ns12.9 coding region caused a slight reduction in Rluc or ns12.9-Rluc sg mRNA level during infection (Fig. 2G). This result indicated that the Rluc activity differences in the two reporter viruses were not due to the transcription level of sg mRNAs.

Collectively, these results suggested that the ns2 gene is not required for HCoV-OC43 replication and high expression reporter virus can be generated by replacing the ns2 gene with Rluc.

Stability of rHCoVs-OC43 after multiple passages. To examine the *in vitro* stability of the four reporter viruses, rHCoVs-OC43 and HCoV-OC43-WT were passaged 13 times in BHK-21 cells as described above (see Fig. 3A). As shown in Fig. 3B, titers for all viruses increased over the first four passages and became stable in subsequent passages. Moreover, the Rluc activity of rOC43-ns2DelRluc and rOC43-ns12.9StopRluc at each passage showed no significant fluctuations during the passages in BHK-21 cells. However, rOC43-ns2FusionRluc and rOC43-ns12.9FusionRluc showed 4- to 6-fold reduction in Rluc activity during the 13 passages (Fig. 3C). To investigate whether mutations were introduced during the passages, viral RNA was extracted from the supernatant of infected cells of each

327 passage. The Rluc gene and its flanking sequences were detected by RT-PCR.
328 Surprisingly, the Rluc gene remained intact in the genome of all rHCoVs-OC43 as no
329 smaller PCR product was detected over the 13 passages (Fig. 3D). However, sequence
330 analysis of clones of RT-PCR products identified same mutations (two-nucleotide
331 insertion between position 70 and 71), which resulted in a stop codon in the region of
332 the Rluc expression cassette of three rHCoVs-OC43 (see Fig. S1 and Table S2).
333 It is worth mentioning that the replacement of accessory genes with the Rluc gene
334 resulted in rHCoVs-OC43 with higher genetic stability when compared with in-frame
335 insertions of the Rluc gene (Table S2). Because the rOC43-ns2DelRluc showed robust
336 Rluc activity, with little impact on its replication kinetics and it remained genetically
337 stable during 10 passages in BHK-21 cells. We next evaluated the pathogenicity of
338 rOC43-ns2DelRluc in the mouse model. Unlike previously reported ns12.9 deletion
339 mutant (21), the result showed that BALB/c mice inoculated with 100 $TCID_{50}$ of
340 either rOC43-ns2DelRluc or HCoV-OC43-WT showed a severe symptom of twitching
341 limbs at 3 days post-inoculation and caused 100% mortality at 4 days post-inoculation,
342 indicating that deletion of ns2 had no influence on the pathogenicity of
343 rOC43-ns2DelRluc in BALB/c mice (Fig. S2, A and B). Moreover,
344 rOC43-ns2DelRluc remained genetically stable after 5 passages in mice and the viral
345 titers in brain tissues was $10^{7.1}$ $TCID_{50}$/g at 3 days post-inoculation, further confirmed
346 the applicability of rOC43-ns2DelRluc *in vivo* (Fig. S2, D and E).

347 **Suitability of rOC43-ns2DelRluc for high-throughput antiviral drug**
348 **screening.** To verify whether rOC43-ns2DelRluc displayed sensitivity similar to the

parental HCoV-OC43-WT under antiviral drugs treatment, the reporter virus was used to evaluate of the antiviral activity of chloroquine or ribavirin in parallel. As shown in Fig. 4A, chloroquine treatment had a significant inhibitory effect on HCoV-OC43-WT or rOC43-ns2DelRluc replication at low-micromolar concentrations, while ribavirin showed no inhibitory effect at the same concentrations (Fig. 4B). Moreover, a similar decrease in viral copy numbers was observed in the two viruses in the presence of increasing levels of chloroquine or ribavirin, indicating that deletion of the ns2 gene had no effect on the sensitivity of rOC43-ns2DelRluc to the antiviral drugs.

To verify whether the Rluc activity of rOC43-ns2DelRluc could be used for antiviral drug screening, we analyzed the antiviral activity of chloroquine and ribavirin against rOC43-ns2DelRluc in parallel using luciferase-based reporter assays. As expected, Rluc activity was reduced in the presence of increasing levels of chloroquine or ribavirin in a dose-dependent manner (Fig. 4C and Fig. 4D). For chloroquine, an IC_{50} of 0.33 μM and CC_{50} of 397.54 μM was observed (see Table 1), which is in line with a previous report (18). By contrast, ribavirin exhibited an inhibitory effect at concentrations of 3 μM or higher, with an IC_{50} of 10.00 μM and CC_{50} of 156.16 μM (Table 1). Our validation experiments suggested that the rOC43-ns2DelRluc-based Rluc assay allows more sensitive and rapid quantification of viral replication than the traditional quantitative RT-PCR assay, with RLUs of $10^{6.2}$ in dimethyl sulfoxide (DMSO)-treated cells at 72 hpi (data not shown) and the Rluc activity could be detected without extracting viral RNA, suggesting its utility for HTS antiviral drug screening.

371 **Screening for potential host factors that inhibit HCoV-OC43 replication.** To
372 further evaluate the applicability of rOC43-ns2DelRluc for antiviral screening, this
373 reporter virus was employed to screen host factors that inhibit HCoV-OC43
374 replication. Here, we selected eight potential antiviral host factors that were reported
375 against flaviviruses and tested them in RNAi screening. Among these eight host
376 factors, the tripartite motif protein 56 (TRIM56) served as a positive control as it
377 belongs to a new class of host antiviral restriction factors that confers resistance to
378 HCoV-OC43 (25). The effect of knockdown of the individual gene on
379 rOC43-ns2DelRluc replication was expressed as relative luciferase activity (RLA),
380 which is the ratio of RLUs obtained from cells treated with targeting siRNA pools
381 over that obtained from cells that were treated with a control siRNA (26).

382 As expected, compared with HEK-293T cells transfected with a control siRNA,
383 knockdown tripartite motif protein 56 (TRIM56; reduced mRNA levels to 37.2%
384 compared to control cells) increased Rluc activity ~1.62-fold (Fig. 5A). In addition,
385 we showed that knockdown double-stranded RNA-activated protein kinase (PKR) or
386 DEAD-box RNA helicases (DDX3X) could significantly enhance Rluc activity,
387 indicating that PKR and DDX3X are potential anti-HCoV-OC43 host factors (Fig.
388 5A). Moreover, the cell viability assay showed no significant differences between
389 cells transfected with host factor siRNA pools and control cells transfected with
390 scrambled siRNA and efficiency of RNAi-mediated knockdown was assessed using
391 quantitative RT-PCR (Fig. 5B), demonstrating that the validity of these host factors
392 on the replication of the HCoV-OC43.

393 **Validation of PKR and DDX3X as antiviral factors in HCoV-OC43**
394 **replication.** PKR is the strongest antiviral host factor identified in the primary siRNA
395 screening assay. To further validate the antiviral role of PKR in HCoV-OC43
396 replication, Huh7 cells were infected with HCoV-OC43-WT at a MOI of 0.05. Cell
397 pellets were collected at 2, 4, 8, 12 and 24 hpi, respectively. As shown in Fig. 6A,
398 cells infected with HCoV-OC43-WT strongly induced PKR activation at 8 and 12 hpi,
399 which decreased dramatically after 24 hpi. This observation was supported by the
400 detection of phosphorylation of eIF2α, the substrate of phosphorylated PKR, showing
401 high basal levels at 8 and 12 hpi and becoming barely detectable at 24 h (Fig. 6A).
402 These results suggested that phosphorylation of PKR and eIF2α were increased at the
403 early stage of infection, but quickly suppressed at 24 hpi. To determine the role of
404 PKR in HCoV-OC43 replication, Huh7 cells were transfected with PKR-specific
405 siRNAs to knockdown PKR or non-targeting siRNA as a negative control. The results
406 showed that two siRNAs (PKR #2 and PKR#3) efficiently reduced endogenous PKR
407 levels compared to control cells (Fig. 6B). The reduction of endogenous PKR (PKR
408 #2 and PKR#3) resulted in an obvious increase in both HCoV-OC43-WT and
409 rOC43-ns2DelRluc replication with a 1.83-fold increase in Rluc activity or virus titer
410 (Fig. 6C and 6D), indicating that PKR plays an antiviral role in HCoV-OC43-infected
411 cells. The observation of rapid dephosphorylation of eIF-2α in HCoV-OC43-infected
412 cells prompted us to examine the expression of GADD34, which is a component of
413 the protein phosphatase 1 (PP1) complex that dephosphorylates eIF-2α. The mRNA
414 level of GADD34 showed a 5-fold increase in HCoV-OC43-infected Huh7 cells at 24

hpi which served as a feedback loop to mediate eIF-2α dephosphorylation at the corresponding time point (Fig. 6E). Interestingly, we also detected a 1.7-fold induction of the GADD34 mRNA level at 2 hpi, this slight increase of GADD34 mRNA level may play an important role in facilitating HCoV-OC43 replication during its invasion period. Okadaic acid (OA) was defined as a protein phosphatase inhibitor, promoting PKR and eIF2α phosphorylation. To further confirm the effect of PP1 activity on HCoV-OC43 replication, cells were incubated in the presence of OA or DMSO followed by infected with HCoV-OC43-WT or rOC43-ns2DelRluc, respectively. As shown in Fig. 7F, in contrast to DMSO-untreated Huh7 cells, in the presence of different concentrations of OA, the Rluc activity of rOC43-ns2DelRluc was significantly decreased at concentrations of 4 nM, with 10-fold inhibition observed at concentrations of 108 nM. This result was further confirmed by the HCoV-OC43-WT, with obviously reduced virus titers (~11-fold) at concentrations of 108 nM (Fig. 6G). Taken together, these results indicated that PKR and eIF2α phosphorylation induce an antiviral effect in HCoV-OC43-infected cells, and this inhibition was blocked by HCoV-OC43-induced GADD34 expression.

DDX3X is another potent antiviral host factor identified in the siRNA screening assay. Human DDX3X is a newly discovered DEAD-box RNA helicase. In addition to its involvement in protein translation, cell cycle, apoptosis, nuclear export and eukaryotic gene regulation, human DDX3X is a critical molecule in innate immune signaling pathways and contributes to type I interferon (IFN) induction. A previous report showed that DDX3X is upregulated upon DENV or PRRSV infection (27, 28).

437 However, contrary to our expectations, Western blotting showed no change in
438 DDX3X protein levels in Huh7 cells upon HCoV-OC43-WT infection (Fig. 7A). This
439 result was further confirmed by semi-quantitative PCR in HCoV-OC43-WT-infected
440 Huh7 or HEK-293T cells (data not shown). A previous study demonstrated that
441 coexpression of TBK1 with DDX3X rather than overexpression of DDX3X itself led
442 to IFN promoter activation because overexpression of TBK1 causes DDX3X
443 activation (29). Our result showed that silencing of endogenous DDX3X expression
444 using RNAi would significantly affect the transcription level of IFN-β; however,
445 overexpression of DDX3X alone activated the IFN promoter only 2-fold (Fig. 7C and
446 7D). Moreover, the result showed that the Rluc activity of rOC43-ns2DelRluc or virus
447 titers of HCoV-OC43-WT increased by 1.7-fold in DDX3X-silenced cells (DDX3X
448 #1 or DDX3X #3) compared with control cells at 72 hpi (Fig. 7F and 7G).
449 Furthermore, we performed an overexpression assay and demonstrated that
450 overexpression of DDX3X showed antiviral activity against HCoV-OC43 infection
451 (Fig. 7E). Thus, DDX3X may play an antiviral role during HCoV-OC43 infection
452 through positive regulation of innate immune-signaling processes.

453 These data demonstrated the feasibility of using rOC43-ns2DelRluc for drug
454 screening and identifying antiviral host factors.

455

456 **Discussion**

457 Rapid identification of therapeutics is a high priority as there is currently no
458 specific therapy to treat novel *Betacoronavirus* (SARS-CoV and MERS-CoV)

459 infections, which can cause high case-fatality rates (30). A marker virus with the
460 introduction of a reporter gene into the viral genome provides a powerful tool to
461 address this problem. To date, only one reporter HCoV (SARS-CoV-GFP) has been
462 generated and applied to siRNA library screening assay (14). However, the
463 SARS-CoV-GFP lacks sensitivity, as it requires a high infectious dose (MOI of 10)
464 for quantitative screening. Moreover, this reporter virus assay must be performed in a
465 BSL-3 facility, which is costly and labor-intensive. Thus, the generation of a safe and
466 sensitive reporter HCoV for HTS assays is urgent. Here, we reported a sensitive
467 antiviral screening platform based on recombinant HCoV-OC43 (rOC43-ns2DelRluc)
468 that expresses Rluc as a reporter gene. Furthermore, using a luciferase-based siRNA
469 screening assay, we identified two host factors (PKR and DDX3X) that exhibit
470 antiviral effects.

471 HCoV-OC43 encodes two accessory genes, ns2 and ns12.9; however, the
472 biological functions of these HCoV-OC43 accessory genes remain poorly understood.
473 In this study, we generated a variety of luciferase-based rHCoVs-OC43 by genetic
474 engineering of the two accessory genes. Among the rHCoVs-OC43,
475 rOC43-ns12.9StopRluc led to a lower virus yield in BHK-21 cells, suggesting that the
476 ion channel activity of ns12.9 is important for the production of infectious virions. A
477 recent study by Freeman *et al.* showed that in-frame insertion of reporter gene into
478 replicase genes (ns2 or ns3) of murine hepatitis virus (MHV) was tolerated and
479 resulted in similar replication kinetics as MHV-WT (10). These results are consistent
480 with the results obtained by the two Rluc-fusion reporter viruses

(rOC43-ns2FusionRluc and rOC43-ns12.9FusionRluc), which showed replication kinetics similar to HCoV-OC43-WT. However, our study demonstrated that Rluc fused with the accessory genes of HCoV-OC43 was an ineffective way to generate high expressing reporter HCoV because the two Rluc-fusion reporter viruses showed impaired Rluc activity and genetic instability during passages *in vitro*. One reporter virus, rOC43-ns2DelRluc, had similar replication kinetics to the parent virus HCoV-OC43-WT, showing robust Rluc activity during infection of BHK-21 cells. Moreover, deletion of the ns2 gene had no influence on the pathogenicity of rOC43-ns2DelRluc in mice and the inserted Rluc gene remained stable both *in vitro* and *in vivo*. Thus, rOC43-ns2DelRluc might be a superior reporter virus for screening antivirals in terms of growth characteristics, Rluc expression levels and genetic stability.

Recently, a library of FDA-approved drugs used for anti-MERS-CoV screening in cell culture successfully identified four potent inhibitors. Intriguingly, all the screened compounds were broad-spectrum anti-HCoVs drugs that also inhibited the replication of SARS-CoV and HCoV-229E (31). However, the traditional CPE-based viral titration assays were ill-suited for HTS assays as more and more novel antiviral drugs are developed every year. Thus, rOC43-ns2DelRluc would provide a powerful tool for rapid and quantitative screening of broad-spectrum anti-HCoVs drugs. Chloroquine, a clinically approved drug, appeared to be a broad-spectrum CoVs drug, as it blocks the replication of SARS-CoV, HCoV-OC43, MERS-CoV and HCV-229E *in vitro* (32, 33). Additionally, clinical experience gained from treating SARS and

MERS suggested the effectiveness of a number of interventions including ribavirin, interferon (alfacon-1), corticosteroids or a combination of these interventions (34, 35). In our study, rOC43-ns2DelRluc was used to evaluate the antiviral activity of chloroquine and ribavirin in 96-well plates. rOC43-ns2DelRluc with deletion of the ns2 gene showed no impairment in response to drugs treatment compared with HCoV-OC43-WT, showing a similar decrease in viral copy numbers in the presence of increasing concentrations of chloroquine or ribavirin (Fig. 4A and 4B). Moreover, Rluc activity of rOC43-ns2DelRluc was reduced in the presence of increasing levels of chloroquine or ribavirin in a dose-dependent manner, with IC_{50} values similar to those with HCoV-OC43-WT. It is worth mentioning that in our study, we demonstrated that ribavirin exhibited inhibitory effect against HCoV-OC43 only at high concentrations and showed a significant cytotoxicity in BHK-21 cells. These data suggest that rOC43-ns2DelRluc represents a superior model for screening broad-spectrum HCoV drugs without the requirement of BSL-3 confinement.

In the past decade, reporter viruses have been used widely for screening pooled RNAi to discover host factors that can influence the replication of diverse +RNA viruses. Such reporter viruses have allowed sensitive and quantitative evaluation of antiviral or proviral effects (36–40). However, few host factors have been identified that can restrict the replication of CoV. Here, eight potential antiviral host factors in flavivirus infection were selected for RNAi screening using the reporter rOC43-ns2DelRluc, leading to the identification of two anti-HCoV-OC43 host factors (PKR and DDX3X).

525 Many viral families have evolved various regulatory mechanisms that modulate
526 host protein synthesis to maximize the production of progeny viruses. In CoV IBV
527 infection, overexpression of a dominant negative kinase-defective PKR mutant
528 enhanced IBV replication by almost 2-fold (41). In this study, we showed that the
529 basal level of phosphorylated PKR and eIF-2α was unregulated in cells infected with
530 HCoV-OC43 at the early stage of infection. Intriguingly, phosphorylated eIF-2α
531 decreased rapidly via induction of GADD34 expression. Upregulation of eIF-2α
532 phosphorylation using OA significantly reduced HCoV-OC43 replication. These
533 results indicated that PKR plays an antiviral role in HCoV-OC43-infected cells.

534 DDX3X, an alias for DDX3 represented on the X chromosome, belongs to the
535 DEAD-box family of ATP-dependent RNA helicases. It is a multiple-function protein
536 involved in protein translation, cell cycle, apoptosis, nuclear export, translation and
537 assembly of stress granules. There is growing evidence that DDX3X is a component
538 of the innate immune response against viral infections (42). In our study, using RNA
539 interference and overexpression approach, we first described the antiviral role of
540 DDX3X during HCoV-OC43 infection via regulation of the type I IFN pathway.
541 Other studies have suggested that DDX3X is an important host factor required for
542 HCV and HIV infection (43, 44). The core protein of HCV interacts with DDX3X to
543 manipulate splicing and regulation of transcription or translation, and the helicase
544 activity of DDX3X was required for HIV RNA export. Therefore, DDX3X plays
545 distinct roles in virus-specific situations.

546 In summary, we generated a robust and stable luciferase-based recombinant

HCoV-OC43 by replacement of the ns2 gene. This reporter virus can be used for screening anti-HCoVs drugs and host factors. To the best of our knowledge, this is the first construction of a luciferase-based HCoV-OC43 for quantitative antiviral assays. The reporter virus will contribute to future work focused on screening wide-spectrum drugs or host factors influencing HCoV replication.

Acknowledgments

This work was supported by grants from the Megaproject for Infectious Disease Research of China (2014ZX10004001, 2013ZX10004601). The funders had no role in study design, data collection and analysis, decision to publish, or preparation of the manuscript.

Competing Interests

The authors have declared that no competing interests exist.

References

1. **Adams MJ, Lefkowitz EJ, King AM, Carstens EB.** 2014. Ratification vote on taxonomic proposals to the International Committee on Taxonomy of Viruses. Arch Virol **159:**2831–2841.
2. **Perlman S, Netland J.** 2009. Coronaviruses post-SARS: update on replication and pathogenesis. Nat Rev Microbiol **7:**439–450.
3. **Gralinski LE, Baric RS.** 2015. Molecular pathology of emerging coronavirus

infections. J Pathol **235:**185–195.

4. **Desforges M, Le Coupanec A, Stodola JK, Meessen-Pinard M, Talbot PJ.** 2014. Human coronaviruses: viral and cellular factors involved in neuroinvasiveness and neuropathogenesis. Virus Res **194:**145-158.
5. **de Haan CA, Haijema BJ, Boss D, Heuts FW, Rottier PJ.** 2005. Coronaviruses as vectors: stability of foreign gene expression. J Virol **79:**12742–12751.
6. **Stirrups K, Shaw K, Evans S, Dalton K, Casais R, Cavanagh D, Britton P.** 2000. Expression of reporter genes from the defective RNA CD-61 of the coronavirus infectious bronchitis virus. J Gen Virol **81:**1687–1698.
7. **Shen H, Fang SG, Chen B, Chen G, Tay FP, Liu DX.** 2009. Towards construction of viral vectors based on avian coronavirus infectious bronchitis virus for gene delivery and vaccine development. J Virol Methods **160:**48–56.
8. **Bosch BJ, de Haan CA, Rottier PJ.** 2004. Coronavirus spike glycoprotein, extended at the carboxy terminus with green fluorescent protein, is assembly competent. J Virol **78:**7369–7378.
9. **Becares M, Sanchez CM, Sola I, Enjuanes L, Zuñiga S.** 2014. Antigenic structures stably expressed by recombinant TGEV-derived vectors. Virology. **464-465:**274–286.
10. **Freeman MC, Graham RL, Lu X, Peek CT, Denison MR.** 2014. Coronavirus replicase-reporter fusions provide quantitative analysis of replication and replication complex formation. J Virol **88:**5319–5327.

590 **11. Roberts RS, Yount BL, Sims AC, Baker S, Baric RS.** 2006. Renilla luciferase as
591 a reporter to assess SARS-CoV mRNA transcription regulation and efficacy of
592 anti-SARS-CoV agents. Adv Exp Med Biol **581:**597–600.
593 **12. Zhao G, Du L, Ma C, Li Y, Li L, Poon VK, Wang L, Yu F, Zheng BJ, Jiang S,**
594 **Zhou Y.** 2013. A safe and convenient pseudovirus-based inhibition assay to detect
595 neutralizing antibodies and screen for viral entry inhibitors against the novel
596 human coronavirus MERS–CoV. Virol J **10:**266.
597 **13. Cao J, Forrest JC, Zhang X.** 2015. A screen of the NIH Clinical Collection
598 small molecule library identifies potential anti-coronavirus drugs. Antiviral Res
599 **114:**1–10.
600 **14. de Wilde AH, Wannee KF, Scholte FE, Goeman JJ, Ten Dijke P, Snijder EJ,**
601 **Kikkert M, van Hemert MJ.** 2015. A Kinome-Wide Small Interfering RNA
602 Screen Identifies Proviral and Antiviral Host Factors in Severe Acute Respiratory
603 Syndrome Coronavirus Replication, Including Double-Stranded RNA-Activated
604 Protein Kinase and Early Secretory Pathway Proteins. J Virol **89:** 8318–8333.
605 **15. McIntosh K, Becker WB, Chanock RM.** 1967. Growth in suckling-mouse brain
606 of "IBV-like" viruses from patients with upper respiratory tract disease. Proc Natl
607 Acad Sci U S A **58:**2268–2273.
608 **16. St-Jean JR, Jacomy H, Desforges M, Vabret A, Freymuth F, Talbot PJ.** 2004.
609 Human respiratory coronavirus OC43: genetic stability and neuroinvasion. J Virol
610 **78:**8824–8834.
611 **17. Wang F, Chen C, Tan W, Yang K, Yang H.** 2016. Structure of Main Protease

612 from Human Coronavirus NL63: Insights for Wide Spectrum Anti-Coronavirus
613 Drug Design. Sci Rep **6:**22677.

614 **18. Keyaerts E, Li S, Vijgen L, Rysman E, Verbeeck J, Van Ranst M, Maes P.**
615 2009. Antiviral activity of chloroquine against human coronavirus OC43 infection
616 in newborn mice. Antimicrob Agents Chemother **53:**3416–3421.

617 **19. Jacomy H, Fragoso G, Almazan G, Mushynski WE, Talbot PJ.** 2006. Human
618 coronavirus OC43 infection induces chronic encephalitis leading to disabilities in
619 BALB/C mice. Virology **349:**335–346.

620 **20. Mounir S., Labonte P. & Talbot P. J.** 1993. Characterization of the nonstructural
621 and spike proteins of the human respiratory coronavirus OC43: comparison with
622 bovine enteric coronavirus. Adv Exp Med Biol **342:**61–67.

623 **21. Zhang R, Wang K, Ping X, Yu W, Qian Z, Xiong S, Sun B.** 2015. The ns12.9
624 accessory protein of human coronavirus OC43 is a viroporin involved in virion
625 morphogenesis and pathogenesis. J Virol **89:**11383–11395.

626 **22. St-Jean JR, Desforges M, Almazán F, Jacomy H, Enjuanes L, Talbot PJ.** 2006.
627 Recovery of a neurovirulent human coronavirus OC43 from an infectious cDNA
628 clone. J Virol **80:**3670–3674.

629 **23. Reed LJ, Münch HA.** 1938. Simple method of estimating fifty percent endpoints.
630 Am J Hyg **27:**493–497.

631 **24. Hu Q, Lu R, Peng K, Duan X, Wang Y, Zhao Y, Wang W, Lou Y, Tan W.** 2014.
632 Prevalence and genetic diversity analysis of human coronavirus OC43 among
633 adult patients with acute respiratory infections in Beijing. PLoS One **9:**e100781.

634 **25. Liu B, Li NL, Wang J, Shi PY, Wang T, Miller MA, Li K.** 2014. Overlapping
635 and distinct molecular determinants dictating the antiviral activities of TRIM56
636 against flaviviruses and coronavirus. J Virol **88:**13821–13835.
637 **26. Jiang D, Weidner JM, Qing M, Pan XB, Guo H, Xu C, Zhang X, Birk A,**
638 **Chang J, Shi PY, Block TM, Guo JT.** 2010. Identification of five
639 interferon-induced cellular proteins that inhibit west nile virus and dengue virus
640 infections. J Virol **84:**8332-8341.
641 **27. Li G, Feng T, Pan W, Shi X, Dai J.** 2015. DEAD-box RNA helicase DDX3X
642 inhibits DENV replication via regulating type one interferon pathway. Biochem
643 Biophys Res Commun **456:**327–332.
644 **28. Chen Q, Liu Q, Liu D, Wang D, Chen H, Xiao S, Fang L.** 2013. Molecular
645 cloning, functional characterization and antiviral activity of porcine DDX3X.
646 Biochem Biophys Res Commun **443:**1169–1175.
647 **29. Soulat D, Bürckstümmer T, Westermayer S, Goncalves A, Bauch A,**
648 **Stefanovic A, Hantschel O, Bennett KL, Decker T, Superti-Furga G.** 2008.
649 The DEAD-box helicase DDX3X is a critical component of the TANK-binding
650 kinase 1-dependent innate immune response. EMBO J **27:**2135–2146.
651 **30. Falzarano D, de Wit E, Martellaro C, Callison J, Munster VJ, Feldmann H.**
652 2013. Inhibition of novel β coronavirus replication by a combination of
653 interferon-α2b and ribavirin. Sci Rep **3:**1686.
654 **31. de Wilde AH, Jochmans D, Posthuma CC, Zevenhoven-Dobbe JC, van**
655 **Nieuwkoop S, Bestebroer TM, van den Hoogen BG, Neyts J, Snijder EJ.** 2014.

Antimicrobial Agents and Chemotherapy

656 Screening of an FDA-approved compound library identifies four small-molecule
657 inhibitors of Middle East respiratory syndrome coronavirus replication in cell
658 culture. Antimicrob Agents Chemother **58:**4875–4884.

659 **32. Keyaerts E, Vijgen L, Maes P, Neyts J, Van Ranst M.** 2004. In vitro inhibition
660 of severe acute respiratory syndrome coronavirus by chloroquine. Biochem
661 Biophys Res Commun **323:**264–268.

662 **33. Kono M, Tatsumi K, Imai AM, Saito K, Kuriyama T, Shirasawa H.** 2008.
663 Inhibition of human coronavirus 229E infection in human epithelial lung cells
664 (L132) by chloroquine: involvement of p38 MAPK and ERK. Antiviral Res
665 **77:**150–152.

666 **34. Gross AE, Bryson ML.** 2015. Oral Ribavirin for the Treatment of Noninfluenza
667 Respiratory Viral Infections: A Systematic Review. Ann Pharmacother **49:**1125–
668 1135.

669 **35. Groneberg DA, Poutanen SM, Low DE, Lode H, Welte T, Zabel P.** 2005.
670 Treatment and vaccines for severe acute respiratory syndrome. Lancet Infect Dis
671 **5:**147–155.

672 **36. Karlas A, Machuy N, Shin Y, Pleissner KP, Artarini A, Heuer D, Becker D,**
673 **Khalil H, Ogilvie LA, Hess S, Mäurer AP, Müller E, Wolff T, Rudel T, Meyer**
674 **TF.** 2010. Genome-wide RNAi screen identifies human host factors crucial for
675 influenza virus replication. Nature **463:**818–822.

676 **37. Hao L, Sakurai A, Watanabe T, Sorensen E, Nidom CA, Newton MA,**
677 **Ahlquist P, Kawaoka Y.** 2008. Drosophila RNAi screen identifies host genes

important for influenza virus replication. Nature **454:**890–893.

38. **Zhou H, Xu M, Huang Q, Gates AT, Zhang XD, Castle JC, Stec E, Ferrer M, Strulovici B, Hazuda DJ, Espeseth AS.** 2008. Genome-scale RNAi screen for host factors required for HIV replication. Cell Host Microbe **4:**495–504.

39. **Krishnan MN, Ng A, Sukumaran B, Gilfoy FD, Uchil PD, Sultana H, Brass AL, Adametz R, Tsui M, Qian F, Montgomery RR, Lev S, Mason PW, Koski RA, Elledge SJ, Xavier RJ, Agaisse H, Fikrig E.** 2008. RNA interference screen for human genes associated with West Nile virus infection. Nature **455:**242–245.

40. **Sessions OM, Barrows NJ, Souza-Neto JA, Robinson TJ, Hershey CL, Rodgers MA, Ramirez JL, Dimopoulos G, Yang PL, Pearson JL, Garcia-Blanco MA.** 2009. Discovery of insect and human dengue virus host factors. Nature **458:**1047–1050.

41. **Wang X, Liao Y, Yap PL, Png KJ, Tam JP, Liu DX.** 2009. Inhibition of protein kinase R activation and upregulation of GADD34 expression play a synergistic role in facilitating coronavirus replication by maintaining de novo protein synthesis in virus-infected cells. J Virol **83:**12462-12472.

42. **Schröder M, Baran M, Bowie AG.** 2008. Viral targeting of DEAD box protein 3 reveals its role in TBK1/IKKepsilon-mediated IRF activation. EMBO J **27:**2147–2157.

43. **Pène V, Li Q, Sodroski C, Hsu CS, Liang TJ.** 2015. Dynamic Interaction of Stress Granules, DDX3X, and IKK-α Mediates Multiple Functions in Hepatitis C Virus Infection. J Virol **89:**5462–5477.

700 **44. Yedavalli VS, Neuveut C, Chi YH, Kleiman L, Jeang KT.** 2004. Requirement
701 of DDX3 DEAD box RNA helicase for HIV-1 Rev-RRE export function. Cell
702 **119:**381–392.

703

704

705 **Figure legends**

706

707 **Fig. 1. Development of human coronaviruses-OC43 (HCoV-OC43) reporter**
708 **systems.** Schematic representation of the cDNA clone pBAC-OC43^{FL} and
709 recombinant cDNA clones of HCoV-OC43 harboring the Renilla luciferase (Rluc)
710 gene, which was introduced into the accessory genes by overlapping polymerase
711 chain reaction (PCR) as described in the Materials and methods. The Rluc gene (green)
712 is depicted. Expanded regions show the transcription regulatory sequence (TRS)
713 control of Rluc gene expression.

714

715 **Fig. 2. Characterization of reporter viruses using engineered accessary genes.** (A)
716 The N protein of recombinant HCoVs-OC43 (rHCoVs) examined by indirect
717 immunofluorescence assay (IFA). At 72 h postinfection, virus-infected BHK-21 cells
718 were incubated with anti-OC43-N mouse polyclonal antibodies and then stained with
719 fluorescein isothiocyanate (FITC)-labeled goat anti-mouse IgG. Cells were analyzed
720 under a fluorescence microscope. (B) Growth kinetics of rHCoVs. BHK-21 cells were
721 infected with rHCoVs and HCoV-OC43-WT at a multiplicity of infection (MOI) of

722 0.01. Viral titers from culture supernatants at the indicated time points were
723 determined by indirect IFA. Data represent three independent experiments and are
724 shown as means ± standard deviation. (C) Complementation of rOC43-ns2DelRluc
725 infection in BHK-21 cells expressing ns2. Cells were transfected with a plasmid
726 expressing ns2-EGFP or a control vector using the X-tremeGENE HP DNA
727 Transfection Reagent, and the expression levels of ns2-EGFP were analyzed by
728 Western blot using anti-GFP antibody (left). After 24 h post-transfection, BHK-21
729 cells were infected with HCoV-OC43-WT or rOC43-ns2DelRluc at an MOI of 0.01.
730 Cell supernatants were collected at 72 h post-infection, and the viral titers were
731 determined by IFA (right). (D) Time-course analysis of the reporter gene expression.
732 The Rluc activity represented as relative light units (RLU) was measured in BHK-21
733 cells infected with rHCoVs at the indicated time points (MOI = 0.01). Data represent
734 three independent experiments and are shown as means ± standard deviation. (E and F)
735 Western blot analysis of reporter gene expression. Proteins in cell lysates of BHK-21
736 cells infected with rHCoVs and HCoV-OC43-WT were analyzed by Western blot
737 using anti-OC43-N, anti-Rluc and anti-β-actin antibodies. Cell lysates from
738 uninfected cells (Mock) served as a negative control. (G) The effect of inserted
739 reporter gene on subgenomic (sg) RNA synthesis. 72 h post-infection (MOI = 0.01),
740 total cellular mRNAs were extracted and subjected to RT-PCR to determine the
741 mRNA level of ns2 (HCoV-OC43-WT), Rluc (rOC43-ns2DelRluc and
742 rOC43-ns12.9StopRluc), ns2-Rluc (rOC43-ns2FusionRluc) and ns12.9-Rluc
743 (rOC43-ns12.9FusionRluc). HCoV-OC43-WT was used as control. Data were

744 normalized to the levels of internal mouse GAPDH mRNA. Error bars indicate means
745 and standard deviations of three independent experiments.
746
747 **Fig. 3. Analysis of genetic stability of the reporter viruses.** (A) Illustration of the
748 virus passage procedure in BHK-21 cells. rHCoVs rescued from transfected cells
749 were defined as P0. Culture supernatants from the transfected cells (P0) were added to
750 näive cells to obtain passage 1 virus (P1). After 13 rounds of serial passages, the
751 reporter viruses were passaged to P13. (B) Viral titers of reporter viruses during
752 passages. Reporter viruses were passaged 13 times in BHK-21 cells, and the
753 supernatants were collected from the virus-infected cells of each passage and titrated
754 using the IFA-based viral titration assay. Data represent three independent
755 experiments and are shown as means ± standard deviation. (C) Rluc activity of
756 reporter viruses of each passage. BHK-21 cells were infected with reporter viruses
757 (MOI = 0.01) of each passage in 48-well plates and assayed for the Rluc activity in
758 RLUs at 72 h post-infection. Data represent mean values of three independent
759 experiments with error bars representing the standard deviations of the means. (D)
760 Analysis of genetic stability of the reporter viruses after several passages in BHK-21
761 cells. Viral RNA was extracted from culture supernatants of each passage, and
762 RT-PCR was performed with a primer set flanking the Rluc gene. The resulting
763 RT-PCR products were resolved by 1% agarose gel electrophoresis.
764
765 **Fig. 4. Replication of HCoV-OC43 in response to drugs treatment in BHK-21**

766 **cells.** (A and B) Effect of chloroquine or ribavirin on the replication of
767 HCoV-OC43-WT or rOC43-ns2DelRluc. BHK-21 cells seeded in 48-well plates were
768 infected with HCoV-OC43-WT or rOC43-ns2DelRluc at an MOI of 0.01 for 2 h and
769 subsequently treated with chloroquine or ribavirin at the indicated concentrations. At
770 72 h post-infection, supernatants were removed and subsequently analyzed for viral
771 load by real time quantitative RT-PCR. Error bars indicate means and standard
772 deviations of three independent experiments. (C and D) Chloroquine or ribavirin
773 inhibition of Rluc activity of rOC43-ns2DelRluc and cell cytotoxic effects. The
774 inhibition assay was performed as described in the Materials and methods. Rluc
775 activity of chloroquine- or ribavirin-treated cells was normalized to dimethyl
776 sulfoxide (DMSO)-treated control cells and measured relative to DMSO-treated cells.
777 Viable cell numbers were used to determine the percentage cytotoxic effect in
778 drug-treated cells relative to DMSO-treated cells. Error bars indicate means and
779 standard deviations of three independent experiments. (E and F) The antiviral effect of
780 chloroquine or ribavirin on HCoV-OC43-WT N protein synthesis.
781
782 **Fig. 5. Screening of host factors influencing HCoV-OC43 replication using**
783 **rOC43-ns2DelRluc.** (A) HEK-293T cells were transfected with various small
784 interfering RNA **(**siRNA) pools, followed by infection with rOC43-ns2DelRluc at an
785 MOI of 0.01 in 48-well plates, and assayed for Rluc activity. The relative luciferase
786 activity (RLA) represents the mean ± the standard deviation (n = 3) of the ratio of
787 relative light units (RLUs) obtained from cells treated with targeting siRNAs to the

RLUs obtained from cells that were treated with a nontargeting siRNA (siControl), which had no adverse effect on the viruses and cells. (B) Real-time RT-PCR was used to quantitate the knockdown effect of the indicated siRNA pools at 36 h post-transfection (gray bars) and the effect of siRNA transfection on cell viability was analyzed in parallel (black bars), and values were normalized to those of nontargeting siRNA-transfected cells (100%). Error bars indicate means and standard deviations of three independent experiments. *, $P < 0.05$; **, $P < 0.01$.

Fig. 6. Validation of PKR as an antiviral factor in HCoV-OC43 replication. (A) HCoV-OC43 infection induced the phosphorylation of PKR and eIF2α. Huh7 cells were infected with HCoV-OC43 or mock infected at an MOI of 0.05 and harvested at 2, 4, 8, 12 and 24 hpi. The cell lysates were collected and analyzed by Western blot with anti-PKR, anti-p-PKR, anti-eIF2α, and anti-p-eIF2α (S51) antibodies. β-actin was used as a protein loading control. (B) Knockdown of PKR expression at 48 h post transfection. (C and D) Knockdown PKR induced the replication of HCoV-OC43 in Huh7 cells. The Rluc activity of rOC43-ns2DelRluc and titers of HCoV-OC43-WT were determined at 72 hpi. Data represent three independent experiments and are shown as means ± standard deviation. (E) Induction of GADD34 expression in HCoV-OC43-infected Huh7 cells at 12 h post infection. (F and G) Reduction of HCoV-OC43 replication by inhibition of PP1 activity with okadaic acid (OA) in HCoV-OC43-infected Huh7 cells. Huh7 cells were treated with OA or DMSO after infected with rOC43-ns2DelRluc or HCoV-OC43-WT. The Rluc activity of

rOC43-ns2DelRluc and titers of HCoV-OC43-WT were determined at 72 hpi. Data represent three independent experiments and are shown as means ± standard deviation. *, $P < 0.05$; **, $P < 0.01$.

Fig. 7. Validation of DDX3X as an antiviral factor in HCoV-OC43 replication. (A) The expression level of DDX3X was unchanged in HCoV-OC43-infected Huh7 cells. Huh7 cells were infected with HCoV-OC43 or mock infected at an MOI of 0.05 and harvested at 2, 4, 8, 12 and 24 hpi. Cell lysates were collected and analyzed by Western blot with anti-DDX3X antibody. β-actin was used as a protein loading control. (B and C) DDX3X is required for IFN-β induction. siRNA-treated HEK-293T cells were infected with Sendai virus (Sev). Induction of IFN-β mRNA was measured by semi-quantitative PCR. (D) Overexpression of DDX3X alone was insufficient to activate the IFN promoter. HEK-293T cells were transfected with 500 ng of plasmids encoding DDX3X or TBKI, co-transfected with plasmids TBK1 (500 ng) and DDX3X (100 or 300 ng), together with 500 ng of IFN-β-Luc reporter plasmid and an internal control plasmid pRL-TK (20 ng) as indicated. (E) Overexpression of DDX3X showed weak antiviral activity against HCoV-OC43. Huh7 cells were transfected with pFlag-DDX3X or empty vector. 24 h post-transfection, cells were infected with HCoV-OC43 an MOI of 0.05 and titers of HCoV-OC43-WT were determined at 72 hpi. (F and G) siRNA-mediated DDX3X silencing induced HCoV-OC43 replication. The Rluc activity of rOC43-ns2DelRluc and titers of HCoV-OC43-WT were determined at 72 hpi. Data represent three independent experiments and are shown as

832 means ± standard deviation. *, $P < 0.05$; **, $P < 0.01$.

Figure 1

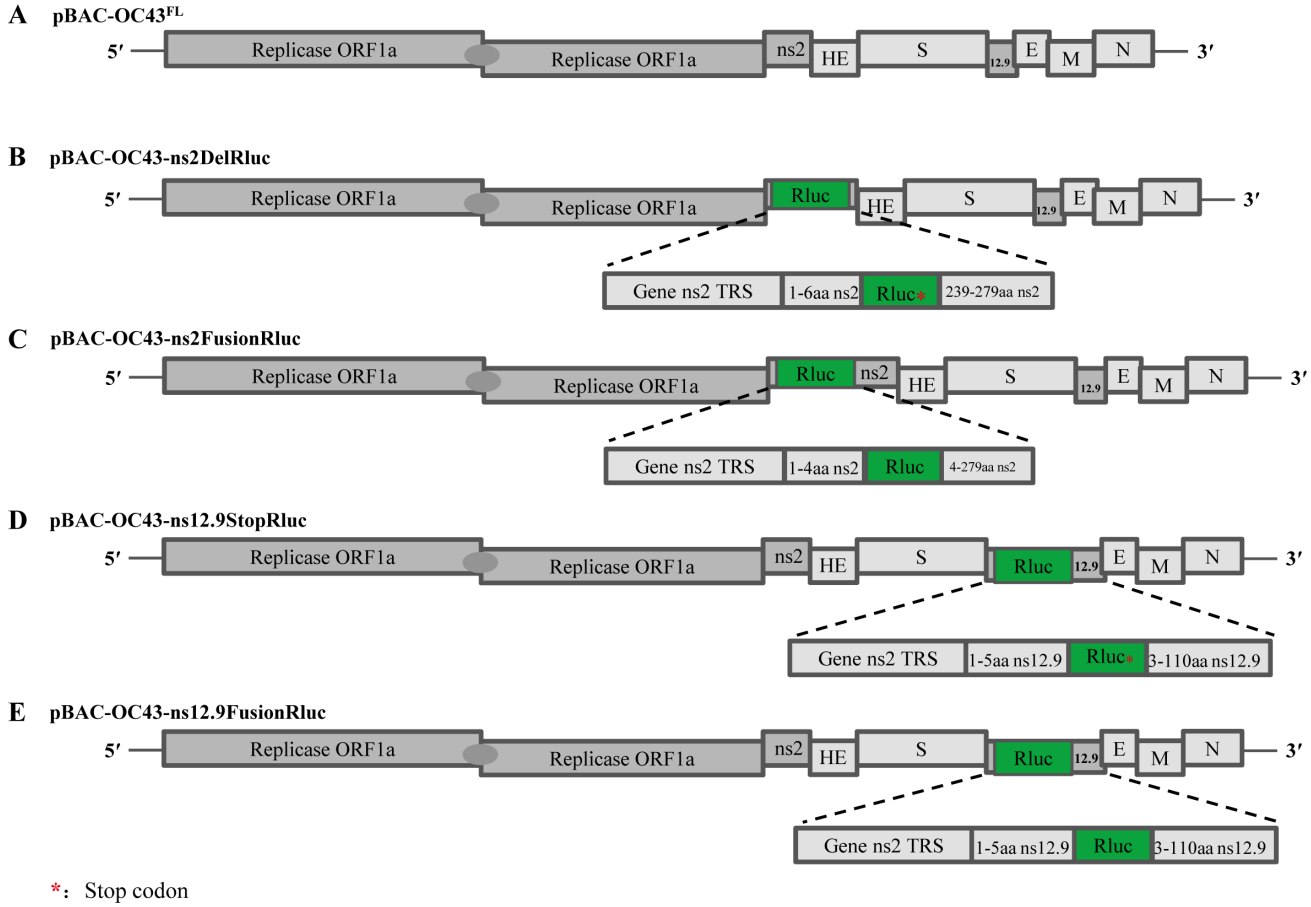

*: Stop codon

Figure 2

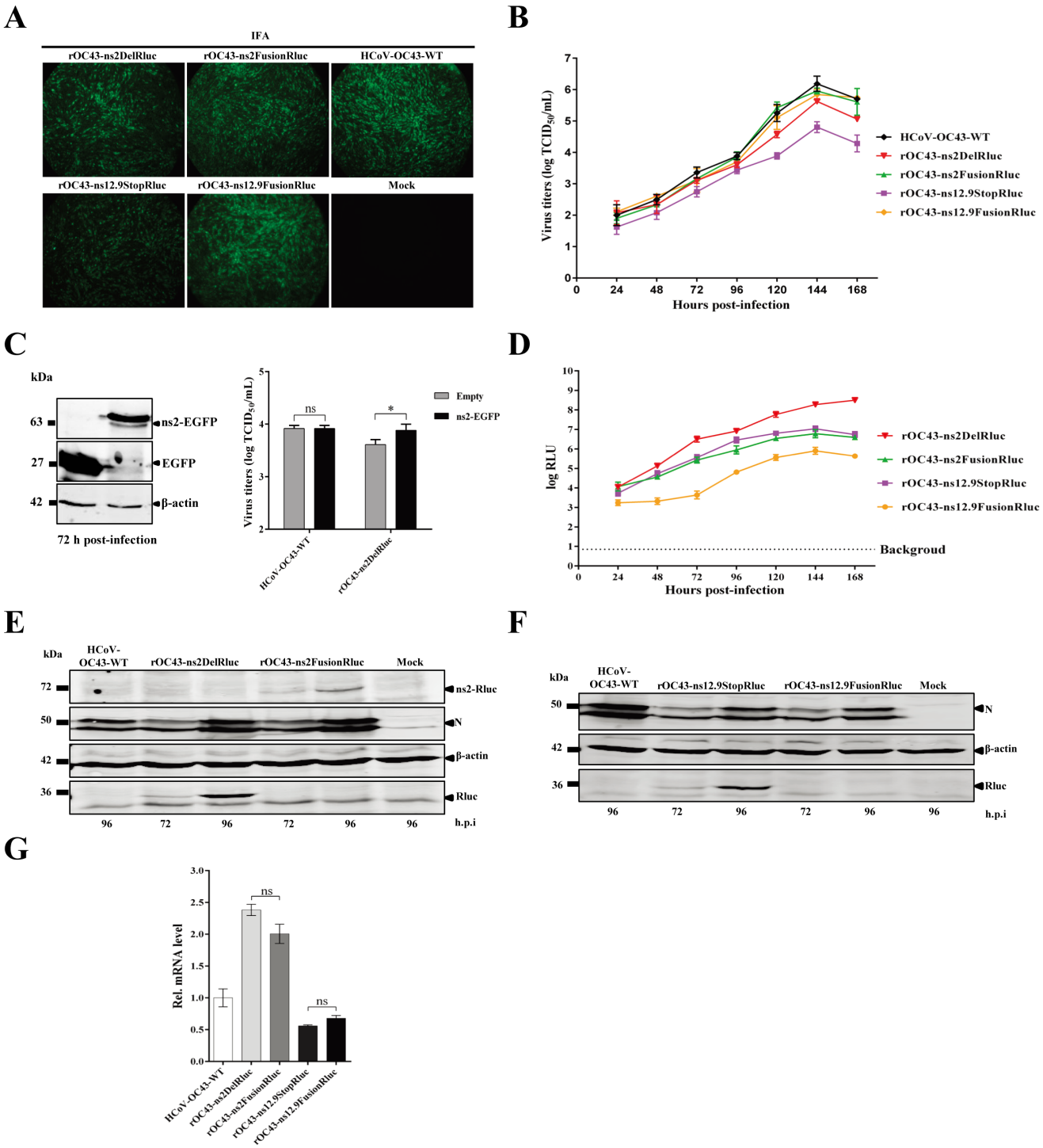

Figure 3

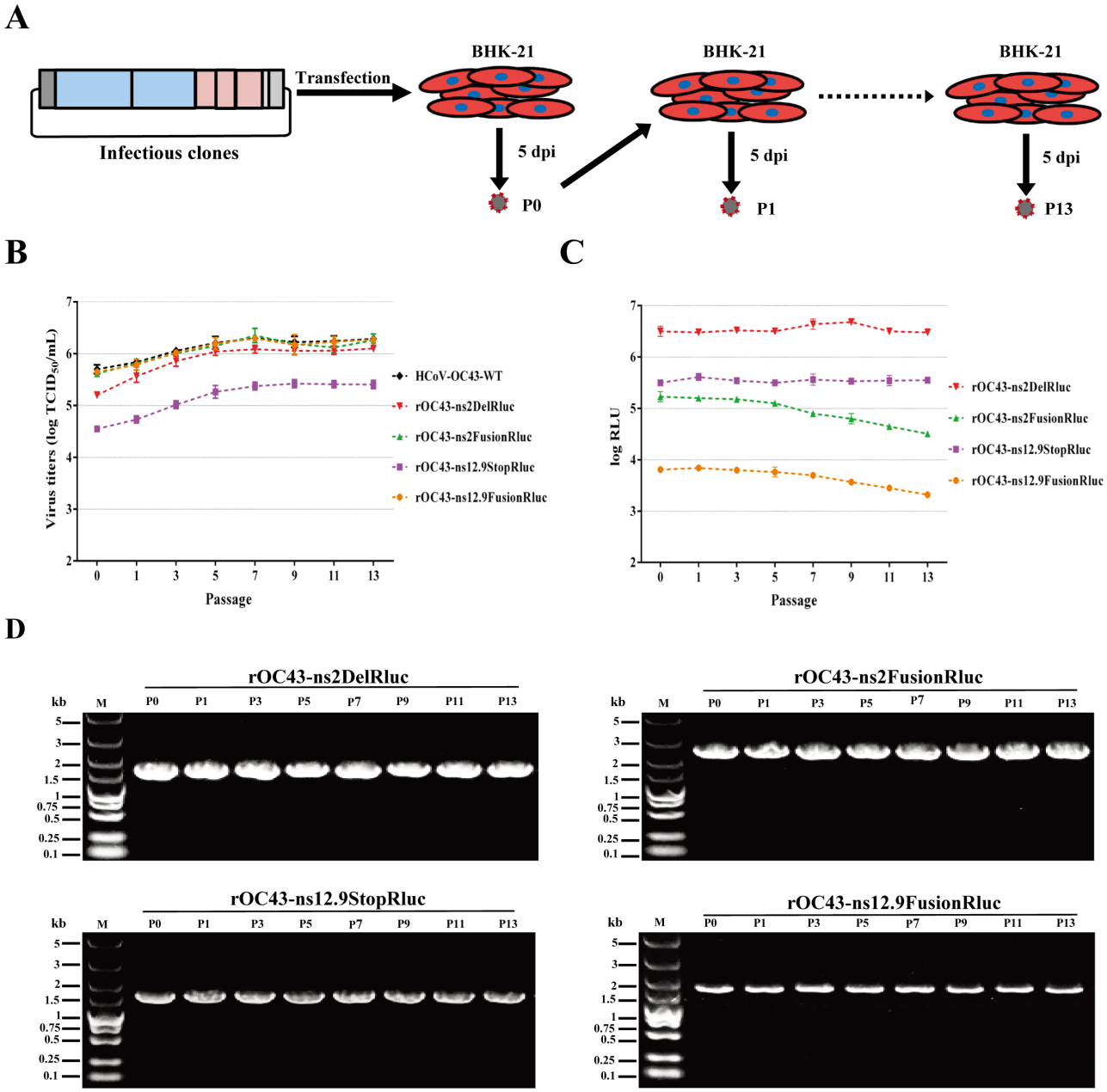

Figure 4

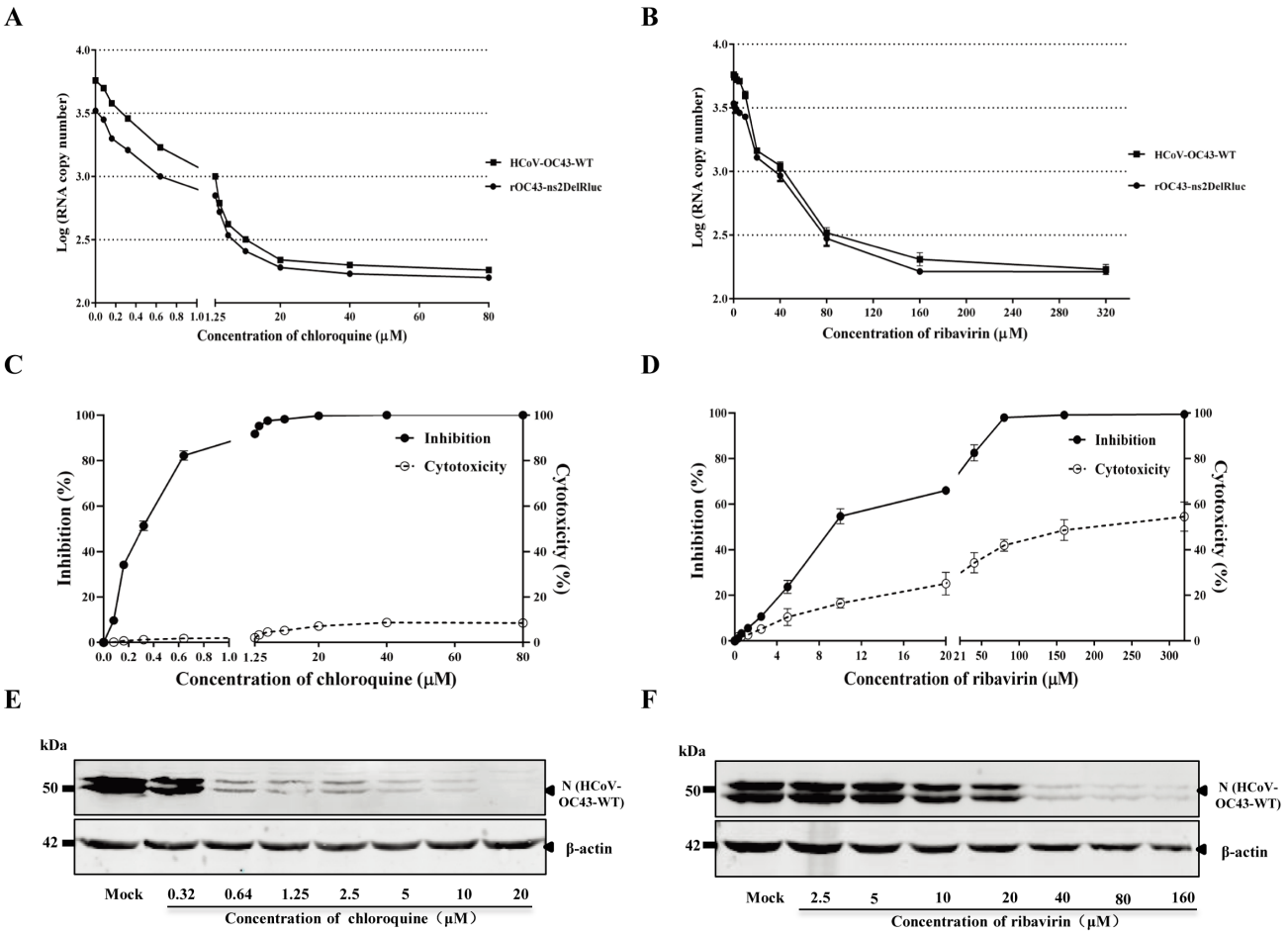

Figure 5

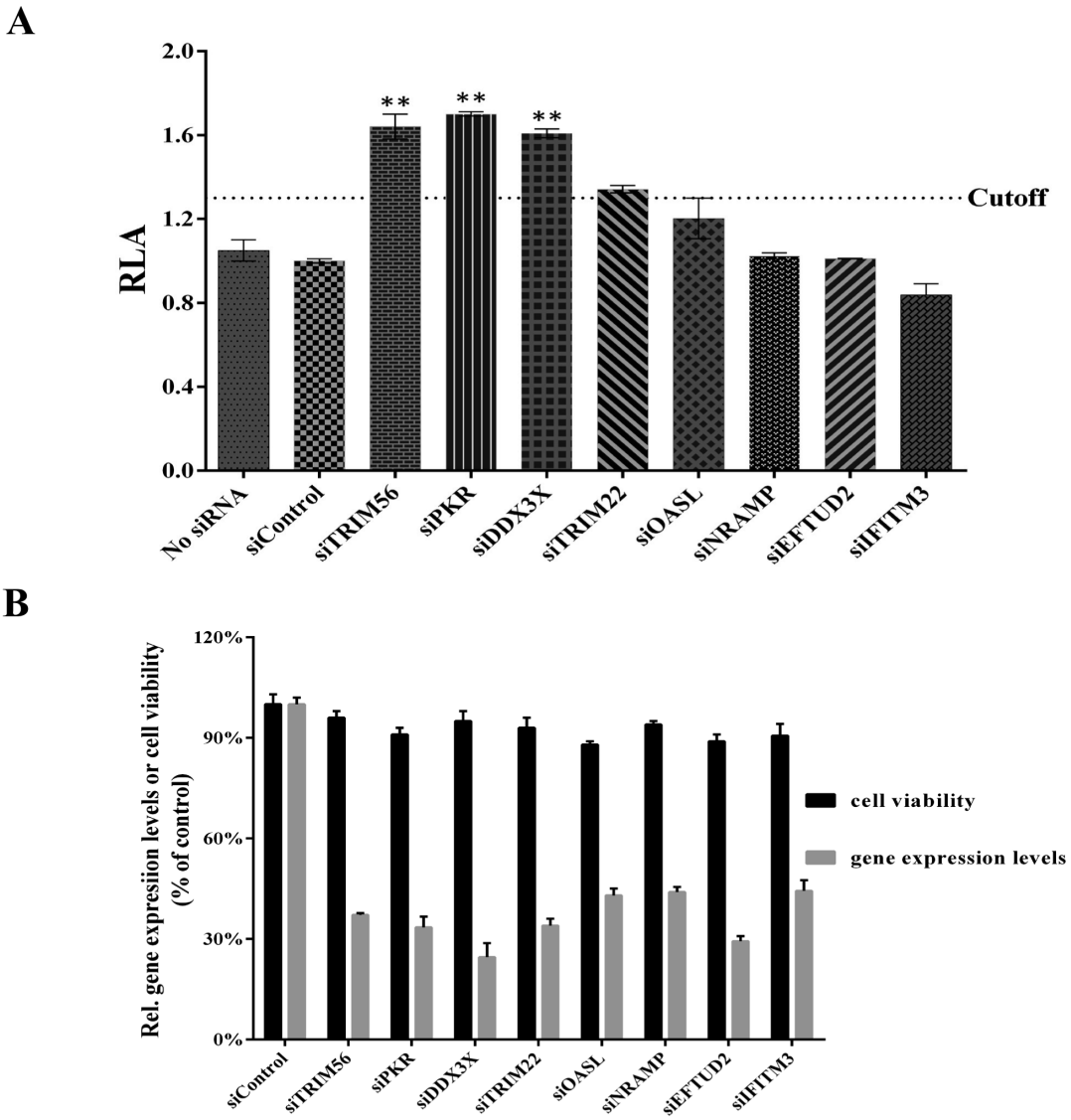

Figure 6

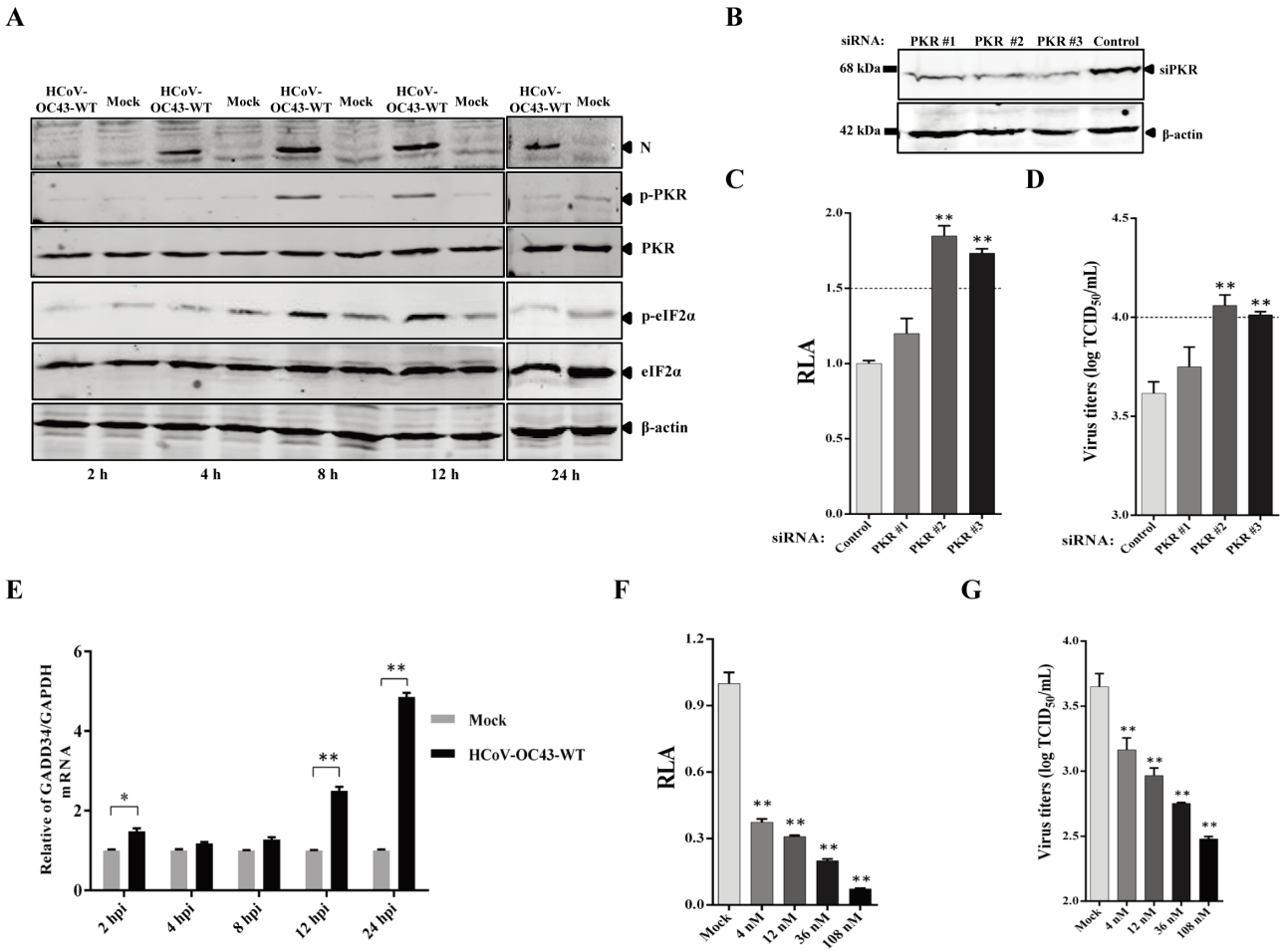

Figure 7

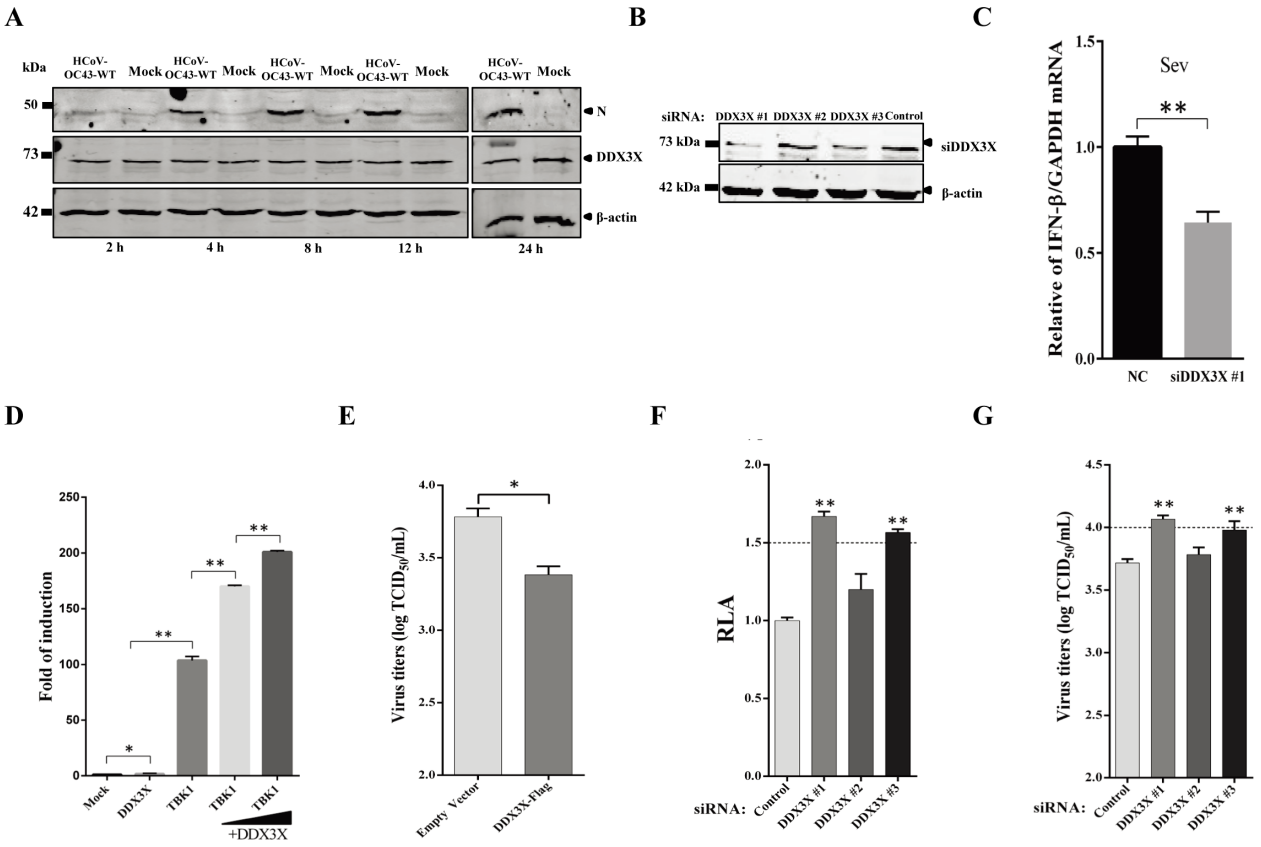

TABLE 1. Antiviral activity of chloroquine or ribavirin in BHK-21 cells

Drugs	CC_{50}, µM	IC_{50}, µM
Chloroquine	397.54	0.33
Ribavirin	156.16	10.00

Data represent mean values for three independent experiments. IC50, 50% effective concentration of chloroquine or ribavirin for the inhibition of rOC43-ns2DelRluc. CC50, 50% cytotoxic concentration of chloroquine or ribavirin for mock-infected BHK-21 cells.